THE JOURNAL OF PHYSICAL CHEMISTRY B

Article

pubs.acs.org/JPCB

NMR Investigation of Exchange Dynamics and Binding of Phenol and Phenolate in DODAC Vesicular Dispersions

Paolo Sabatino,*[,†,‡] Rudra Prosad Choudhury,[§,⊥] Monika Schönhoff,[§] Paul Van der Meeren,[†] and José C. Martins[‡]

[†]Particle and Interfacial Technology Group, Faculty of Bioscience Engineering, Ghent University, Coupure Links 653, B-9000 Gent, Belgium

[‡]NMR and Structure Analysis Unit, Department of Organic Chemistry, Faculty of Sciences, Ghent University, Krijgslaan 281 S4, B-9000 Gent, Belgium

[§]Institute of Physical Chemistry, University of Muenster, Corrensstr. 28-30, D-48149 Münster, Germany

ABSTRACT: The interaction between phenol molecules, both in their undissociated and dissociated states, and cationic dioctadecyl dimethylammonium chloride (DODAC) vesicles were thoroughly investigated using NMR techniques. In particular, diffusion and relaxation measurements, combined with the two sites Kärger model, were used to evaluate the exchange dynamics and the binding of the aromatic molecules to the vesicles. The results reveal that, besides concentration and vesicle preparation method, pH conditions have the biggest impact on the phenol sorption behavior. Although the dissociated form of phenol formed at high pH is more hydrophilic, the results indicated that phenol–DODAC interactions were largely favored in basic conditions as a consequence of the strong electrostatic interaction between the phenolate anions and the cationic surfactant headgroup.

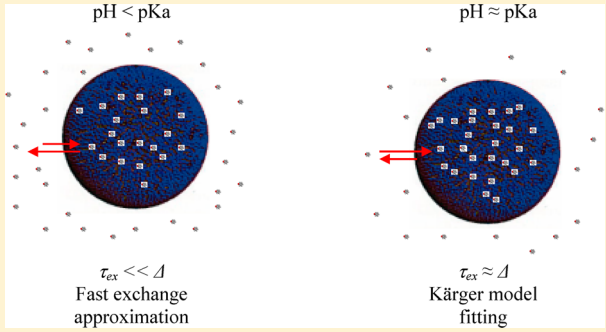

INTRODUCTION

Cationic dioctadecyl dimethylammonium chloride molecules (DODAC), in aqueous solution, show the ability to self-assemble to form molecular aggregates consisting of one or several curved bilayer shells entrapping a portion of water in the inner core. Because of this particular structure, these aggregates, known as vesicles, possess the capacity to incorporate both hydrophilic (in the aqueous core) and hydrophobic (in the bilayers) solutes.[1] This amphiphilic behavior allows vesicles to be used as a model system for biological membranes.[2,3]

The uptake and release of hydrophobic components by lipid membranes is an important research topic in diverse areas. Cellular uptake of drugs is strongly influenced by their interaction with the cellular membranes.[1,4,5] Also the toxic effects of endocrine disruptors can to a large extent be ascribed to their interaction with cell membranes. Hereby, there is a growing body of evidence that simple characteristics such as the octanol/water partition coefficient are not sufficient to predict interaction of chemicals with membranes.[6] In addition, sorption of sparingly water-soluble compounds from an aqueous matrix in liposomes has been proposed as a promising method in wastewater treatment.[7] Upon sorption, amphiphilic or hydrophobic pollutants can be removed by ultrafiltration. The advantages of liposomes as compared to the more frequently studied micelles are that membranes of large pore size and hence higher flux may be used and that the concentration of dissolved surfactant in the filtrate is much smaller due to the much lower critical aggregation concentration of liposomal surfactants. It follows that the interaction of hydrophobic compounds with bilayers is of great importance from different points of view.

Saveyn et al.[8] investigated the sorption behavior of different benzyl alcohol derivatives in DODAC vesicular dispersions. In their study the authors found that the sorption is largely influenced by the vesicle preparation method (either sonication or extrusion) as well as by temperature. The enhanced solubilization in sonicated cationic vesicles as compared to extruded ones was already described in several papers,[9,10] and it is generally ascribed to the incomplete lipid chain freezing below T_m.[11]

In this contribution, phenol was selected as a model compound in order to enable the variation of the ionization state of the sorbate molecules. Indeed, phenol is not dissociated at neutral pH but becomes negatively charged above its pK_a. Its choice is further motivated by the fact that it has been found as an important contaminant in industrial sites,[12−14] and solubilization can be used to remove phenol and related compounds by soil washing.

In a previous publication,[15] it was noticed that basic pH conditions lead to a significant improvement of the phenol sorption in cationic CTAB micellar solutions, especially when the phenol pK_a was reached and surpassed. Similar findings

Received: May 16, 2012
Revised: June 22, 2012
Published: June 25, 2012

were also reported by Hakimhasemi et al.,[16] studying phenol removal by means of electro-filtration with DODAC dispersions.

Here the solubilization of phenol in DODAC vesicles, either extruded or sonicated, was studied by means of ^{1}H- and pulsed field gradient NMR (PFG-NMR) spectroscopy. The latter allows the determination of the diffusion coefficient of each component of interest from which the partitioning into the lipid bilayer can subsequently be derived, quantitatively, directly in situ in a nondestructive way and without perturbing the equilibrium condition.[8,17−21] In addition, the application of the Kärger two-state model,[22,23] as described by Choudhury and Schönhoff[24] to take into account relaxation effects in different compartments, provided useful information about the exchange dynamics of phenol between the free and bound state, and as consequence allowed us to describe qualitatively the interactions occurring between phenol and surfactant molecules both at neutral and basic pH conditions.

MATERIALS AND METHODS

Materials. Phenol (M_W = 94.11 g/mol, 99% pure) was obtained from Sigma. The cationic surfactant dimethyl dioctadecylammonium chloride (DODAC, M_W = 586.50 g/mol, 97% pure) was purchased from Alfa Aesar (Germany). Sodium hydroxide (M_W = 40 g/mol, 99% pure) was acquired from VWR Prolabo. Deuterium oxide (D_2O >99.8% atomD) was purchased from Armar Chemicals (Switzerland). 4,4-Dimethyl-4-silapentane-1-sulfonate sodium (DSS-d_6, M_W = 224.32 g/mol, >98% atomD) was acquired from Isotec Inc.

Vesicular Dispersion Preparation. 6 mM DODAC dispersions were prepared by first hydrating the lipids in D_2O and stirring at 60 °C (above T_m) during 1 h, using a magnetic stirrer. Subsequently, the dispersions were either sonicated or extruded.

The sonication procedure was carried out using a Sonifier 250 (Branson, Canada) tip sonicator. The 13 mm tip was immersed in 10 mL of vesicular dispersion, approximately two-thirds of the sample height. The power monitor indicated 20%. In the beginning and after every 2 min of sonication, the sample was left to rest in a water bath at 55 °C for 1 min. A 50% duty cycle was selected to prevent heating of the sample. The sonication time was always 10 min in total.

The extrusion procedure was carried out using a TEX060 apparatus (Northern Lipids Inc., Canada), which allows extrusion through 25 mm polycarbonate filters with a 200 nm pore size (Track-Etch; Whatman, U.K.). Hereby, 10 mL of the multilamellar vesicular dispersion was extruded five times through two stacked filters by pressurized nitrogen gas. The resulting dispersion contains mainly unilamellar vesicles.[25] All extrusions were performed at 65 °C, which is far above the gel−liquid-crystalline temperature of the samples (around 41 °C[11]).

Phenol was added to the dispersions, as dry powder, in different concentrations after the sonication and extrusion procedures were finished.

NMR Equipment. All of the NMR experiments were performed on a Bruker Avance II spectrometer operating at a ^{1}H frequency of 700.13 MHz and equipped with a 5 mm ^{1}H TXI-Z gradient probe with a maximum gradient strength of 57.7 G·cm^{-1}. Measurements were performed at 25 °C and the temperature was controlled to within ±0.01 °C with a Eurotherm 3000 VT digital controller.

For chemical shift measurements, a solution of sodium 4,4-dimethyl-4-silapentane-1-sulfonate (DSS-d_6) in D_2O was used as external reference, from which the chemical shift of the residual HDO was determined to be 4.80 ppm at 25 °C. This value was used as secondary reference throughout all measurements.

Diffusion measurements were carried out using a stimulated echo sequence[26] with bipolar sinusoidal shaped gradient pulses, and a double stimulated echo sequence[27] with convection compensation, using monopolar smoothed rectangular shaped gradient pulses and a modified phase cycle to minimize phase distortions due to unwanted gradient echos.[28] The echo decay of the resonance intensity obtained obeys eq 1, from which it is clear that the diffusion coefficient D is derived from the echo-decay as a function of the parameter k

$$I(k) = I_0 \exp(-Dk) \tag{1}$$

where k is expressed in eqs 2 and 3 for bipolar and monopolar sequences,[29] respectively

$$k = \gamma^2 g^2 \delta^2 \frac{4}{\pi^2}\left(\Delta - \frac{5\delta}{16} - \frac{\tau_g}{2}\right) \tag{2}$$

$$k = \gamma^2 g^2 \delta^2 0.9(\Delta - 0.6\delta) \tag{3}$$

where I is the echo intensity with gradient, I_0 is the echo intensity at zero gradient, D is the diffusion coefficient, γ is the gyromagnetic ratio, g is the maximum gradient amplitude, δ is the duration of the gradient pulse, Δ is the diffusion delay, and τ_g is the gradient pulse recovery delay of the bipolar pairs.

The T_2 relaxation experiments were carried out using the Carr−Purcell−Meiboom−Gill (CPMG) sequence [90°−(τ−180°−τ)$_n$], whereas T_1 relaxation times were measured by inversion recovery experiments [180°−τ−90°].

Dynamic Light Scattering. Dynamic light scattering experiments were performed using a photon correlation spectrometer (PCS 100, Malvern Instruments Ltd., U.K.) with a 10 mW helium−neon laser (Melles Griot, The Netherlands). All measurements were performed at 25 °C at a scattering angle of 90°. Cumulant analysis was employed to calculate the harmonic intensity-weighted average hydrodynamic particle diameter and the polydispersity index. Typically, five independent measurements were taken to obtain a mean hydrodynamic diameter and polydispersity.

pH Measurements. pH measurements were performed using a HI 9126 portable pH/ORP meter (Hanna Instruments, U.S.A.). All measurements were performed at room temperature.

THEORETICAL BACKGROUND

Determination of the Partitioning into the Vesicles. When phenol molecules are added to a vesicular dispersion of DODAC surfactant, they are either dissolved in water or solubilized in the vesicles. In the former state, phenol diffuses freely in the aqueous phase, whereas upon sorption, the phenol molecules diffuse together with the surfactant aggregates. Since phenol molecules are present in two different sites, it follows that these molecules will be characterized by different values of diffusion coefficients and relaxation times for the free state (D_f, T_{1f}, and T_{2f}) and for the bound state (D_b, T_{1b}, and T_{2b}). Under these conditions the intensity of the echo-decay cannot be described by eq 1, but it is rather expressed as a superposition of exponentials.

Since in such a system molecular exchange between free and bound states is possible, the Kärger model,[22,23] conveniently

modified to take into account relaxation rates,[24,30] must be applied and eq 1 must be rewritten as

$$\frac{I}{I_0}(k) = P_1 \exp(-kD_1) + P_2 \exp(-kD_2) \tag{4}$$

where D_1 and D_2 are the apparent self−diffusion coefficients defined below and P_1 and P_2 are the normalized populations. The apparent self-diffusion coefficients are linked to the diffusion coefficients of the free and bound species, D_f and D_b, respectively, by

$$D_{1,2} = \frac{1}{2}\left\{(D_f + D_b) + \frac{\Delta}{k}\left(\frac{1}{T_f} + \frac{1}{T_b} + \frac{1}{\tau_f} + \frac{1}{\tau_b}\right) \mp \left(\left[(D_b - D_f) + \frac{\Delta}{k}\left(\frac{1}{T_b} - \frac{1}{T_f} + \frac{1}{\tau_b} - \frac{1}{\tau_f}\right)\right]^2 + \frac{4\Delta^2}{k^2\tau_b\tau_f}\right)^{1/2}\right\} \tag{5}$$

while the prefactors are given by

$$P_1 = 1 - P_2 \tag{6a}$$

$$P_2 = \frac{1}{(D_2 - D_1)}\left\{P_f\left(D_1 + \frac{\Delta}{kT_b}\right) + P_b\left(D_2 + \frac{\Delta}{kT_b}\right) - D_1\right\} \tag{6b}$$

where P_f and P_b are the population fractions expressed as

$$P_b = \frac{\tau_b}{\tau_f + \tau_b} \tag{7a}$$

$$P_f = \frac{\tau_f}{\tau_f + \tau_b} \tag{7b}$$

τ_f and τ_b are the residence times of the phenol molecules in the free and bound state, respectively, and the exchange time between the two sites can be defined as

$$\tau_{ex}^{-1} = \tau_f^{-1} + \tau_b^{-1} \tag{8}$$

In eqs 5 and 6b, T_f and T_b are the effective relaxation times in the free and bound states, respectively, calculated according to the following equation:

$$\frac{1}{T} = \frac{1}{\Delta}\left(\frac{2\tau_1}{T_2} + \frac{\tau_2}{T_1}\right) \tag{9}$$

where τ_1 and τ_2 are the periods of the bipolar stimulated echo pulse sequence: [90°−τ_1/2−180°−τ_1/2−90°−τ_2−90°−τ_1/2−180°−τ_1/2]

The Kärger model provides a general solution for diffusion experiments with exchange occurring between two sites. However, depending on the exchange rate, the Kärger approach can be further simplified. In case of slow exchange (i.e., $\tau \gg \Delta$), eq 4 can be directly rewritten as

$$\frac{I}{I_0}(k) = P_f \exp(-kD_f) + P_b \exp(-kD_b) \tag{10}$$

in which the population fractions and the diffusion coefficients can be obtained by simple biexponential fitting of the echo decay. In case of fast exchange (i.e., $\tau \ll \Delta$), on the other hand, eq 4 reduces to a monoexponential function where the diffusion coefficient observed is a weighted average of the diffusion coefficients of the free and bound species according to eq 11[18]

$$D_{obs} = P_b D_b + (1 - P_b) D_f \tag{11}$$

It is then possible to derive the value of the bound fraction P_b according to

$$P_b = \frac{D_f - D_{obs}}{D_f - D_b} \tag{12}$$

RESULTS AND DISCUSSIONS

Dispersion Characterization. DODAC dispersions were characterized by dynamic light scattering. The hydrodynamic diameters were 66 nm for the sonicated dispersion and 198 nm for the extruded one.

For the sonicated dispersion a broad size distribution is observed (polydispersity index 0.6) as compared to the more narrow size distribution of extruded vesicles (polydispersity index 0.3). Since larger particles scatter more light than smaller particles, the average diameter at 90° is overestimated in polydisperse systems, and as consequence smaller structures might be present for sonicated DODAC dispersions.[31]

Figure 1 shows the ^{1}H NMR spectra of 6 mM DODAC dispersions in D_2O at 25 °C. Whereas the measurements are performed below T_m, still liquid state spectral contributions of the lipid resonances are clearly visible for the sonicated dispersion (Figure 1a). This has been attributed by Saveyn et al.[11] to the partial fluid character of sonicated vesicles below T_m. The resonance at 0.93 ppm belongs to the two terminal methyl groups of the alkyl chains. The intense resonance at 1.35 ppm is representative of the aliphatic methylene groups, whereas the smaller ones at 1.69 and 3.30 ppm belong to β and α methylene groups, respectively. The single resonance at 3.18 ppm originates from the two methyl groups attached to the quaternary ammonium group.

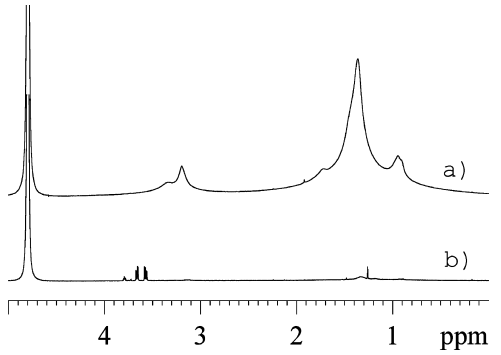

Figure 1. ^{1}H NMR spectra of 6 mM DODAC sonicated (a) and extruded (b) dispersions in D_2O at 25 °C.

The NMR spectrum of extruded vesicles (Figure 1b), on the other hand, does not display any of the characteristic resonances of the surfactant. The bigger size and the more rigid character of extruded vesicles below T_m, lead to a more efficient relaxation causing line broadening beyond detection in the spectrum.

The two dispersions were further characterized by diffusion NMR experiments which allowed the estimation of the enclosed volume analyzing the echo decay of the water signal.[32]

In the presence of extruded vesicles, the water signal shows a biexponential echo-decay, suggesting that the exchange time between the internal and external water compartments is slow as compared to the diffusion time used (Δ = 100 ms). In this

dx.doi.org/10.1021/jp304749g | J. Phys. Chem. B 2012, 116, 9269−9276

case the internal water fraction can be estimated by biexponential fitting which gave a value of the enclosed volume of about 4%.

In the presence of sonicated vesicles, on the other hand, the water signal shows a monoexponential echo-decay, pointing out the faster exchange between the water pools, which is a logical consequence of the more liquid-like nature of the bilayer of the sonicated vesicles. Under these circumstances the internal water fraction can be calculated using eq 12 in which D_f is the diffusion of external water, which is assumed to diffuse as free water (1.9×10^{-9} m^2 s^{-1}), D_{obs} is the value obtained experimentally (1.8×10^{-9} m^2 s^{-1}) and D_b is the diffusion coefficient of water in the internal compartments, which can be neglected since it is at least 2 orders of magnitude smaller than D_f (due to restricted diffusion). The calculated internal fraction is about 5%. However, this latter value is expected to be slightly overestimated because of the obstruction effect, whereby the water in the external phase is not completely free, but experiences the presence of the vesicles, which slightly reduces its diffusional speed. In conclusion, the water diffusion data reveal that only a minor (negligible) fraction of water (and hence of water-dissolved species) is present within the vesicles.

Sorption Determination. Figure 2a shows the ^{1}H NMR spectrum of 6 mM phenol in D_2O at 25 °C. The doublet at

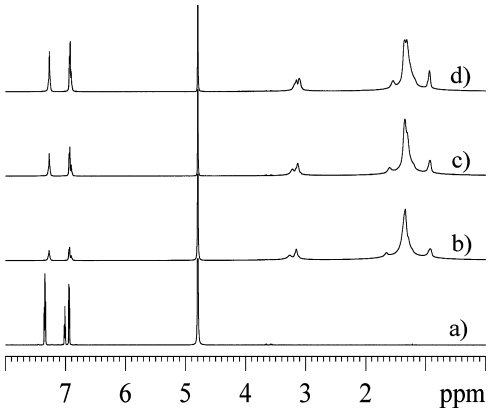

Figure 2. ^{1}H NMR spectra of (a) 6 mM phenol in D_2O and (b–d) phenol 3, 6, and 10 mM and 6 mM sonicated DODAC in D_2O at 25 °C.

6.96 ppm represents the ortho-protons, while the two triplets at 7.03 and 7.36 ppm belong to para- and meta-protons, respectively. Figure 2b–d illustrates the spectrum of the sample containing phenol at different concentrations and 6 mM sonicated DODAC vesicles in D_2O at 25 °C. In all cases the aromatic region displays two instead of three resonances for the phenol, a simplification resulting from the overlap of the ortho and para resonances. Moreover, the two resonances are shifted toward higher fields (shift >0.07 ppm) and broadened, whereby the ortho-protons apparently shift less compared to the meta and para-protons. This is interpreted as signifying that these remain most in contact with external water upon sorption. The chemical shift variation and the broadening effect are an indication that the phenol is at least partially absorbed in the vesicular bilayer. Since a single set of resonances is observed, this suggests fast exchange of phenol between the aqueous phase and the vesicular bilayer on the time scale given by the difference of the resonance frequencies.

In the surfactant region, a perturbation to lower values of the chemical shift (upfield) for the α-, β-methylene groups as well as the $-N^+(CH_3)_2$ group was noticed. This upfield shift is most likely attributed to ring current shift effects[15,33] caused by phenol. The long alkyl chain and the terminal methyl group resonances, on the other hand, were only slightly affected by the presence of phenol. The variation of chemical shift of the surfactant resonances is summarized in Table 1.

Table 1. Chemical Shift Variation of Sonicated Surfactant Moieties in the Presence of Phenol at Different Concentrations[a]

	chemical shift variation (ppm)				
phenol [mM]	CH_3	$(CH_2)_n$	β-CH_2	$N^+(CH_3)_2$	α-CH_2
0	0.95	1.37	1.73	3.20	3.35
3	−0.02	−0.03	−0.08	−0.05	−0.08
6	−0.02	−0.02	−0.13	−0.06	−0.13
10	−0.01	−0.04	−0.19	−0.09	−0.20

[a]Negative values indicate a shift towards lower values of chemical shift in ppm.

Although it is not possible to assess the binding site of phenol within the vesicles in more detail, the chemical shift perturbations noticed for both the aromatic molecule and for the lipid headgroup do suggest the presence of a cation–π interaction.[15,21,33]

Similar series of experiments were carried out with phenol in the presence of 6 mM extruded DODAC dispersion as shown in Figure 3. Although no information can be obtained about the

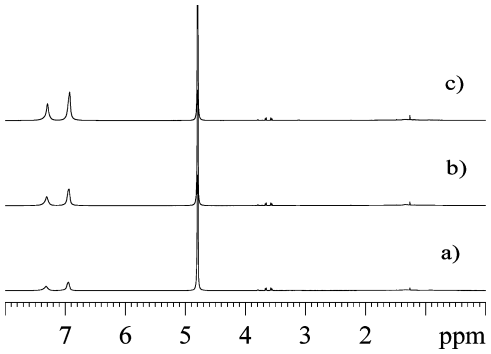

Figure 3. ^{1}H NMR spectra of phenol (a) 3, (b) 6, and (c) 10 mM and 6 mM extruded DODAC in D_2O at 25 °C.

surfactant behavior due to the extreme line broadening, the aromatic region is characterized by two phenol resonances, as already seen for the case of sonicated vesicles, and an even more pronounced broadening effect. Moreover, also in these conditions a shift of the resonances toward higher fields is observed, even if the variation is clearly less distinct. The observation that the chemical shift variation is reduced for extruded vesicles indicates there is less sorption than in the sonicated vesicles.[8–10]

In order to evaluate the fraction of phenol sorbed by the lipid, PFG-NMR measurements were carried out using the modified Kärger model to fit the data. This model requires a set of diffusion experiments recorded with different diffusion delays (from 100 to 1000 ms): the analysis of the echo-decays of these experiments, using eqs 4–6 and 9 allows the estimation of unknown parameters (T_{2b}, τ_b, τ_f and T_{1b}) provided that a set of

dx.doi.org/10.1021/jp304749g | J. Phys. Chem. B 2012, 116, 9269–9276

fixed input parameters are known (D_f, D_b, T_{1f}, and T_{2f}). The fraction of sorbed phenol and the exchange time between the two sites are calculated from the residence times according to eqs 7 and 8.

In our case D_f, T_{1f}, and T_{2f} are the diffusion coefficient, the spin−lattice and spin−spin relaxation times of free phenol, respectively. Since these values were found not to be significantly affected by phenol concentration, in the concentration range used here (3−10 mM), their average values were used for the fitting procedure: $D_f = (7.4 \pm 0.1) \times 10^{-10}$ m^2/s, $T_{1f} = (7.6 \pm 0.3)$ s, and $T_{2f} = (4.9 \pm 0.3)$ s.

For the diffusion coefficient of phenol in the bound state, the diffusion coefficient of the vesicle itself is taken, as determined by dynamic light scattering. The values are $D_b = (6.0 \pm 0.2) \times 10^{-12}$ m^2/s and $D_b = (2.0 \pm 0.2) \times 10^{-12}$ m^2/s for sonicated and extruded vesicles, respectively. The error is estimated by repeating the DLS measurements five times.

Figure 4 shows some typical echo decay curves as function of diffusion time together with the Kärger model fit for a sample

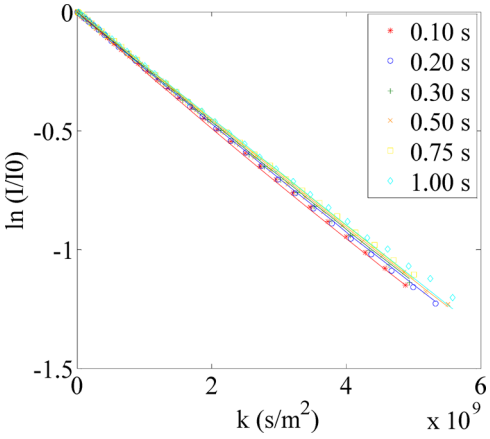

Figure 4. Echo−decay of 6 mM phenol in a 6 mM sonicated DODAC dispersion in D_2O at 25 °C for different values of the diffusion time Δ as indicated. The markers represent the experimental data points while the line represents the Kärger model fit.

containing 6 mM phenol and 6 mM sonicated DODAC. The parameters of the best fitting model are reported in Table 2.

The values summarized in Table 2 indicate that the sorption degree depends on the DODAC/phenol concentration ratio. For the sonicated dispersion, the sorption is higher at low concentrations of phenol while at higher phenol concentrations the vesicles become saturated and more phenol is present free in solution. Hence, deviations from a pure partitioning model occur. In fact, these experimental data fit a Langmuir model (r^2 = 0.9894) from which the sorption maximum and affinity parameter were estimated to be 1.44 mol phenol/mol DODAC and 0.11 (mM phenol)$^{-1}$, respectively. On the basis of the concentrations of phenol analyzed (3, 6, and 10 mM), the percentage of bound phenol, and the DODAC concentration (6 mM), the molar ratio of bound aromatic molecules per DODAC molecule in sonicated vesicles was 0.23, 0.40, and 0.60 in the presence of 3, 6, and 10 mM phenol, respectively.

Table 2 also summarizes the values of sorption for extruded dispersions, from which it is clear that, at lower concentration of phenol added, the sorption into the sonicated dispersion was higher than in the extruded dispersion confirming the qualitative indication of the chemical shift variation. Moreover, Table 2 shows that the sorption for extruded dispersions is less dependent on phenol/DODAC concentration ratio. In particular, the sorption remains constant with phenol concentration, meaning that extruded vesicles are not completely saturated and that sorption is a cooperative effect whereby the membrane fluidization introduced by sorption further stimulates additional sorption.[8] In this case, the molar ratio of bound phenol to DODAC was 0.17, 0.36, and 0.63 for 3, 6, and 10 mM phenol concentration, respectively.

In both cases, the relaxation times, spin−lattice and spin−spin, are strongly shortened for the sorbed phenol when compared to the relaxation times for free phenol. In particular, the relaxation time T_{2b} is only some ms, i.e., more than 3 orders of magnitude shorter than the value measured for free phenol, which indicates that the molecular motion of phenol is dominated by the bilayer upon sorption.

As far as the exchange time τ_{ex} is concerned, the fitted values are in the order of a few milliseconds, but are characterized by a large confidence interval. However, even taking the confidence interval into account, it can be safely stated that the exchange rate is fast as compared to the diffusion time scale ($\tau_{ex} \ll \Delta$). For the sake of completeness, it can be mentioned that the diffusion controlled exchange dynamics can be estimated based on Schonhoff and Soderman work,[34] which yields exchange times of 0.06·Pb/(1-Pb) ms and 0.19·Pb/(1-Pb) ms for the sonicated and extruded vesicles, respectively. Hence, the exchange dynamics of sorbed phenol in DODAC vesicles are about an order of magnitude slower as compared to the diffusion controlled case. On the other hand, the exchange time of the sorbed phenol in DODAC dispersions was an order of magnitude faster as compared to the exchange time of phenol sorbed in polyelectrolytes capsules.[24]

The confidence intervals were estimated by varying the input parameters in their error range and checking the influence on the fitted parameters. This procedure revealed that the fitting is only sensitive to the diffusion coefficient of free phenol D_f, while T_{1f} and T_{2f} had hardly any effect on the fitted parameters.

However, because the confidence interval estimation is exclusively obtained varying the input parameters, they only represent a part of the total error. To further check the reliability of the Kärger model in this fast exchange condition, the phenol sorption was also estimated by using eq 12. Table 3 shows the results obtained following the fast exchange approximation.

D_{obs} is the diffusion coefficient for phenol in the presence of DODAC obtained by a single diffusion experiment, with a

Table 2. Best Fitting Parameters of the Kärger Model Applied to the Echo Decay Curves of Phenol in 6 mM DODAC at 25 °C

	T_{1b} (s)		T_{2b} (ms)		τ_{ex} (ms)		P_b (%)	
phenol [mM]	extrusion	sonication	extrusion	sonication	extrusion	sonication	extrusion	sonication
3	0.5 ± 0.1	0.6 ± 0.2	1.2 ± 0.0	2.3 ± 0.1	3.4 ± 0.2	7.1 ± 2.4	34 ± 1	45 ± 1
6	0.5 ± 0.2	0.6 ± 0.3	1.0 ± 0.2	2.6 ± 0.1	1.8 ± 0.3	6.6 ± 1.5	36 ± 1	40 ± 1
10	0.5 ± 0.2	0.6 ± 0.3	1.0 ± 0.1	3.0 ± 0.2	5.2 ± 0.7	5.9 ± 1.6	38 ± 1	36 ± 1

dx.doi.org/10.1021/jp304749g | J. Phys. Chem. B 2012, 116, 9269−9276

Table 3. Diffusion Coefficients of Phenol in the Presence (D_{obs}) and the Absence (D_f) of 6 mM DODAC Dispersion at 25 °C as well as Sorbed Fraction

phenol [mM]	D_f [10^{-10} m^2/s]	D_{obs} [10^{-10} m^2/s]		sorption [%]	
		extrusion	sonication	extrusion	sonication
3	7.4 ± 0.1	5.0 ± 0.1	3.9 ± 0.1	32 ± 3	47 ± 3
6	7.4 ± 0.1	4.9 ± 0.1	4.2 ± 0.1	34 ± 3	43 ± 3
10	7.4 ± 0.1	4.8 ± 0.1	4.6 ± 0.1	35 ± 3	38 ± 3

diffusion delay of 1.0 s, in which the echo decay was fitted by a monoexponential function. The term P_bD_b is neglected, because D_b was 2 orders of magnitude smaller than D_f. The values of the percentage of sorption were not significantly different from the ones found using the Kärger model, although the confidence interval is larger.

Table 3 summarizes the D_{obs} values and the sorption fractions estimated from diffusion experiments in which the diffusion delay was set to 1.0 s, since in this condition the fast exchange approximation is best fulfilled ($\tau_{ex} \ll \Delta$). However, due to the very rapid exchange dynamics, the values of D_{obs} are found to be only slightly dependent on the diffusion delay used and a reliable estimation of the sorbed fraction can be also obtained from a single diffusion experiment with the shorter diffusion delays of 100 ms ($\tau_{ex} < \Delta$).

pH Effect. As phenol dissociates with increasing pH, resulting in anionic phenolate ions, two opposing effects will occur. First of all, the phenolate ion is much more hydrophilic, which is expected to have a negative impact on sorption, on the other hand, electrostatic interactions between anionic solute and cationic surfactant might favor sorption. To assess the impact of the phenol ionization state on the interaction with DODAC vesicles, ^{1}H NMR spectra were recorded, where the pH was varied by addition of sodium hydroxide. Whereas the pK_a of phenol in water is reported to be 9.99,[35] the corresponding value in D_2O is 10.30, when determined as shown by Krezel and Bal.[36] Figure 5 shows the ^{1}H NMR spectra of 6 mM phenol and 6 mM sonicated DODAC in D_2O at 25 °C in a pH range between 8.8 and 12.2. The pH value for an analogous sample without addition of sodium hydroxide was found to be 7.8 and its ^{1}H NMR spectrum is shown in Figure 5a.

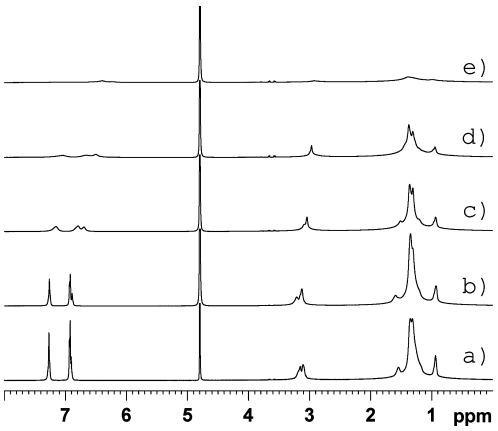

Figure 5. ^{1}H NMR spectra of 6 mM phenol and 6 mM sonicated DODAC in D_2O at 25 °C at different pH conditions: (a) 7.8, (b) 8.8, (c) 9.4, (d) 10.5, and (e) 12.2.

From Figure 5, the influence of pH on the phenol-DODAC interactions it is clearly visible. The spectrum recorded at pH 8.8 (Figure 5b) is substantially unvaried as compared to the one registered at pH 7.8, whereas already at pH 9.4 (Figure 5c), i.e., slightly below the phenol pK_a, the aromatic signals are further shifted toward lower ppm values and also the resonances of the lipid head groups display a similar trend. Moreover, under these conditions, the phenol signals are much broader, meaning that the relaxation time and, hence, the rotational mobility of the molecules is largely reduced. Jointly considering all these effects suggests that at higher pH conditions either a larger amount and/or a larger binding strength of phenol sorbed into the vesicle bilayers is obtained. The latter can be ascribed to the presence of the phenolate anion ($C_6H_5O^-$) that, being negatively charged, more favorably interacts with the positively charged surfactant head by electrostatic interaction.

Increasing the pH of the solution, this effect is even more prominent. At pH 10.5 (Figure 5d) the intensity of the phenol resonances is strongly reduced and the two peaks become very broad. For what concerns the surfactant region, a further variation in chemical shift is observed for the $-N(CH_3)_2$ signal while no shift is visible for both alkyl chain and terminal methyl group resonances. At pH 12.2 (Figure 5e) the two aromatic signals are hardly visible and also the surfactant signals display a consistent broadening effect. The latter phenomenon is due to the neutralization of the vesicles (in this pH condition) that leads to the formation of bigger vesicles which are characterized by shorter relaxation times. This growth upon pH rising was also confirmed by supplementary dynamic light scattering measurements. In these conditions, the average hydrodynamic diameter was 546 nm with a polydispersity index of 0.5.

Similar studies were performed for extruded dispersions. However, it was observed that phenol resonances already completely disappear around pH 9, i.e., below the phenol pK_a and as a consequence the effect of phenol ionization could not be investigated.

In order to quantitatively estimate the sorption as a function of pH, the Kärger model has been used. The reason why the Kärger model is preferred to the more straightforward fast exchange approach is that at higher pH, it might be expected that electrostatic attraction between the oppositely charged species leads to stronger binding, probably characterized by a longer exchange time τ_{ex}. However, due to the almost complete loss of the aromatic signals at higher pH (10.5 and 12.2), diffusion experiments could only be carried out for the samples at pH 8.8 and 9.4.

The model input parameters for the sample at pH 9.4 are slightly different from the ones used for the sample at pH 7.8 and are listed below: $D_f = [7.1 \pm 0.1]10^{-10}$ m^2/s, $T_{1f} = [6.4 \pm 0.3]$ s, and $T_{2f} = [4.2 \pm 0.2]$ s, whereas for the sample at pH 8.8 the same input parameters as for sample at pH 7.8 were applied. Figure 6 displays the echo decay curves as a function of diffusion time together with the Kärger model fit for the sample at pH 9.4.

The parameters obtained by means of Kärger fitting for the samples at pH 7.8, 8.8 (echo decays not shown), and 9.4 are summarized in Table 4.

At this higher pH condition the Kärger approach reveals that the amount of phenol sorbed into the vesicles is significantly higher than in neutral pH conditions. Moreover, the exchange rate between phenol molecules in the free and sorbed sites is now much slower and it is of the same order of magnitude as

dx.doi.org/10.1021/jp304749g | J. Phys. Chem. B 2012, 116, 9269−9276

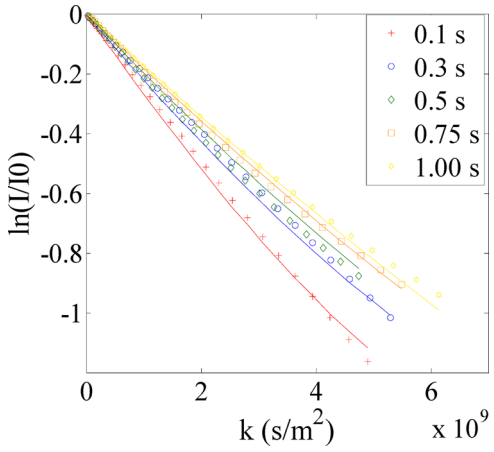

Figure 6. Echo decay of 6 mM phenol in a 6 mM DODAC dispersion in D_2O at pH 9.4 at 25 °C for different values of the diffusion time Δ as indicated. The markers represent the experimental data points while the line represents the Kärger model fit.

Table 4. Best Fitting Parameters of the Kärger Model Applied to the Echo Decay Curves of 6 mM Phenol in 6 mM Sonicated DODAC at Different pH Values at 25 °C

pH	T_{1b} (s)	T_{2b} (ms)	τ_{ex} (ms)	P_b (%)
7.8	0.6 ± 0.3	2.6 ± 0.1	6.6 ± 1.5	40 ± 1
8.8	0.6 ± 0.2	1.6 ± 0.0	24.7 ± 1.5	42 ± 1
9.4	0.6 ± 0.2	1.6 ± 0.1	101.0 ± 6.0	64 ± 1

the diffusion delays used for the diffusion experiments ($\tau_{ex} \approx \Delta$).

Due to slower exchange, it was noticed that, unlike the neutral pH conditions case, the values of observed diffusion coefficients (D_{obs}) estimated from single diffusion experiments were largely dependent on the diffusion delay used. As consequence, under these circumstances, the widely applied fast exchange approach can not be used and reliable results can only be obtained by means of Kärger two region model fitting.

The enhanced sorption and the longer exchange time found, both confirm the higher affinity between phenol and surfactant molecules at high pH, due to the presence of electrostatic interactions that lead to the formation of a stronger sorption as compared to the weaker cation-π interaction present at neutral pH.

Unfortunately, the concomitant decrease in T_{2b} makes the higher pH region experimentally inaccessible.

CONCLUSIONS

The aim of the present paper was to investigate the influence of several factors such as concentration, vesicle preparation methods, and pH on the interaction between phenol and cationic DODAC dispersions, using NMR techniques. In particular, the sorption of phenol in vesicular bilayers was quantitatively estimated by means of pulsed field gradient NMR.

At room temperature the sorption of phenol in its undissociated form was found to be higher in sonicated vesicles than in extruded ones. These findings were explained by the incomplete lipid chain freezing of sonicated dispersions below T_m. As only the chemical shifts of the $N^+(CH_3)_2$, α-CH_2, and β-CH_2 groups were affected by the presence of phenol, it has been hypothesized that phenol molecules were preferentially solubilized close to the positively charged headgroup of the surfactant, pointing toward a cation−π interaction at neutral pH conditions. In addition, exchange between free and sorbed phenol was found to be rapid on the diffusion time scale used.

The influence of the phenol ionization state was investigated by varying the pH conditions. Diffusion experiments at different diffusion delays revealed that the Kärger model was required to prevent unreliable (i.e., apparently diffusion delay dependent) sorption data. The results obtained revealed that in more basic pH conditions the sorbed amount, as well as the exchange time, was considerably larger than at neutral pH. In fact, the exchange time became comparable with the diffusion time at pH values already below the phenol pK_a. Both the enhanced sorption and the longer exchange time indicated a more pronounced interaction between the two species, due to the strong electrostatic attraction between the phenolate anions formed and the cationic vesicles.

AUTHOR INFORMATION

Corresponding Author

*E-mail: Paolo.Sabatino@UGent.be.

Present Address

⊥School of Materials Science and Engineering, Georgia Institute of Technology, Atlanta, Georgia 30332, United States.

Notes

The authors declare no competing financial interest.

ACKNOWLEDGMENTS

The authors thank the Fund for Scientific Research−Flanders (FWO-Vlaanderen) for a Ph.D. fellowship to P.S., as well as for various research and equipment grants (G.0365.03, G.0064.07, G.0678.08, and G.0102.08). The 700 MHz equipment of the Interuniversitary NMR Facility used in this work was financed by UGent, the Free University of Brussels (VUB), and the University of Antwerp (UA) via the "Zware Apparatuur" Incentive of the Flemish Government.

REFERENCES

(1) Lasic, D. D. *Liposomes. From Physics to Applications*; Elsevier: Amsterdam, 1993.
(2) Singer, S. J.; Nicolson, G. R. *Science* **1972**, *175*, 720−731.
(3) Blume, A.; Gabriel, P. Lipid model membranes and biomembranes. In *Handbook of Thermal Analysis and Calorimetry*; Kemp, R. B., Ed.; Elsevier Science: Amsterdam, 1999; Vol. *4*.
(4) Malmsten, M. *Surfactants and Polymers in Drug Delivery*; Marcel Dekker, Inc.: New York, 2002.
(5) Gulati, M.; Grover, M.; Singh, S.; Singh, M. *Int. J. Pharm.* **1998**, *165*, 129−168.
(6) Lukacova, V.; Peng, M.; Tandlich, R.; Hinderliter, A.; Balaz, S. *Langmuir* **2006**, *22*, 1869−1874.
(7) Abe, M.; Kondo, Y. *CHEMTECH* **1999**, *29*, 33−42.
(8) Saveyn, P.; Cocquyt, E.; Sinnaeve, D.; Martins, J. C.; Topgaard, D.; Van der Meeren, P. *Langmuir* **2008**, *24*, 3082−3089.
(9) Lincopan, N.; Mamizuka, E. M.; Carmona-Ribeiro, A. M. *J. Antimicrob. Chemother.* **2003**, *52*, 412−418.
(10) Vieira, D. B.; Pacheco, L. F.; Carmona-Ribeiro, A. M. *J. Colloid Interface Sci.* **2006**, *293*, 240−247.
(11) Saveyn, P.; Van der Meeren, P.; Cocquyt, J.; Drakenberg, T.; Olofsson, G.; Olsson, U. *Langmuir* **2007**, *23*, 10455−10462.
(12) Katsaounos, C. Z.; Paleologos, E. K.; Giokas, D. L.; Karayannis, M. I. *Int. J. Environ. Anal. Chem.* **2003**, *83*, 507−514.
(13) Frenzel, W.; Oleksyfrenzel, J.; Moller, J. *Anal. Chim. Acta* **1992**, *261*, 253−259.

(14) Kang, C. L.; Wang, Y.; Li, R. B.; Du, Y. G.; Li, J.; Zhang, B. W.; Zhou, L. M.; Du, Y. Z. *Microchem. J.* **2000**, *64*, 161−171.
(15) Sabatino, P.; Szczygiel, A.; Sinnaeve, D.; Hakimhashemi, M.; Saveyn, H.; Martins, J. C.; Van der Meeren, P. *Colloids Surf. A, Physicochem. Eng. Asp.* **2010**, *370*, 42−48.
(16) Hakimhashemi, M.; Saveyn, H.; De Bock, B.; Van der Meeren, P. *Chem. Eng. Technol.* **2010**, *33*, 1321−1326.
(17) Stilbs, P. *J. Colloid Interface Sci.* **1982**, *87*, 385−394.
(18) Stilbs, P.; Arvidson, G.; Lindblom, G. *Chem. Phys. Lipids* **1984**, *35*, 309−314.
(19) Momot, K. I.; Kuchel, P. W. *Concepts Magn. Reson.* **2003**, *19A*, 51−64.
(20) Söderman, O.; Stilbs, P.; Price, W. S. *Concepts Magn. Reson.* **2004**, *23A*, 121−135.
(21) Groth, C.; Nyden, M.; Persson, K. C. *Langmuir* **2007**, *23*, 3000−3008.
(22) Kärger, J.; Pfeifer, H.; Heink, W. *Adv. Magn. Reson.* **1988**, *12*, 1−89.
(23) Waldeck, A. R.; Kuchel, P. W.; Lennon, A. J.; Chapman, B. E. *Prog. Nucl. Magn. Reson. Spectrosc.* **1997**, *30*, 39−68.
(24) Choudhury, R. P.; Schönhoff, M. *J. Chem. Phys.* **2007**, *127*, 234702−1−9.
(25) Saveyn, P.; Cocquyt, J.; Frederik, P.; De Cuyper, M.; Van der Meeren, P. *Langmuir* **2007**, *23*, 4775−4781.
(26) Wu, D. H.; Chen, A. D.; Johnson, C. S. *J. Magn. Reson.* **1995**, *115A*, 260−264.
(27) Jerschow, A.; Muller, N. *J. Magn. Reson.* **1997**, *125*, 372−375.
(28) Connell, M. A.; Bowyer, P. J.; Bone, P. A.; Davis, A. L.; Swanson, A. G.; Nilsson, M.; Morris, G. A. *J. Magn. Reson.* **2009**, *198*, 121−131.
(29) Sinnaeve, D. *Concept. Magnetic Res. A* **2012**, *40*, 39−65.
(30) Chakraborty, D.; Choudhury, R. P.; Schönhoff, M. *Langmuir* **2010**, *26*, 12940−12947.
(31) Van De Hulst, H. *Light Scattering by Small Particles*; Dover Publications: New York, 1981.
(32) Sabatino, P.; Saveyn, P.; Martins, J. C.; Van der Meeren, P. *Langmuir* **2011**, *27*, 4532−4540.
(33) Chaghi, R.; de Menorval, L. C.; Charnay, C.; Derrien, G.; Zajac, J. *J. Colloid Interface Sci.* **2008**, *326*, 227−234.
(34) Schönhoff, M.; Söderman, O. *J. Phys. Chem. B* **1997**, *101*, 8237−8242.
(35) Lide, D. R. *Handbook of Chemistry and Physics*, 90th ed.; CRC Press: Boca Raton, FL, 2009.
(36) Krezel, A.; Bal, W. *J. Inorg. Biochem.* **2004**, *98*, 161−166.